

Supplemental Information

**Electrostatic Stabilization of Single-
Atom Catalysts by Ionic Liquids**

Shipeng Ding, Yalin Guo, Max J. Hülsey, Bin Zhang, Hiroyuki Asakura, Lingmei Liu, Yu Han, Min Gao, Jun-ya Hasegawa, Botao Qiao, Tao Zhang, and Ning Yan

Supporting Information

1. Materials and chemicals

Calcium nitrate ($\text{Ca}(\text{NO}_3)_2 \cdot 4\text{H}_2\text{O}$, 99.0%) , ammonium phosphate dibasic ($(\text{NH}_4)_2\text{HPO}_4$, 99.0%), (1,5-Cyclooctadiene)dimethylplatinum(II) (PtCODMe_2 , 97%), platinum(II) acetylacetone($\text{Pt}(\text{acac})_2$), rutile TiO_2 , and CeO_2 were obtained from Sigma-Aldrich. Monoclinic ZrO_2 was supplied by Saint-Gobain NorPro. Hexane (95%), methanol (99.8%), ethanol (absolute) and ammonia solution (25%) were purchased from VWR Chemicals. The 1-Butyl-3-methylimidazolium bis(trifluoromethylsulfonyl)imide ([Bmim][Tf₂N]), 1-Butyl-3-methylimidazolium trifluoromethanesulfonate ([Bmim][CF₃SO₃]) and 1-Butyl-3-methylimidazolium tetrafluoroborate ([Bmim][BF₄]) were purchased from Lanzhou Institute of Chemical Physics, Chinese Academy of Sciences. All chemicals were used as received.

2. Catalyst preparation

2.1 The synthesis of hydroxyapatite ($\text{Ca}_{10}(\text{OH})_2(\text{PO}_4)_6$, HAP)

The support HAP was first prepared using a chemical precipitation method. In a typical synthesis, 11.80 g $\text{Ca}(\text{NO}_3)_2 \cdot 4\text{H}_2\text{O}$ was dissolved in a mixture of 50 mL ethanol and 50 mL DI water in an ice-water bath. The pH value of the solution was adjusted to 11 by adding 25 mL of 25 wt.% ammonia solution, and the solution was stirred for 1 hour. 4.03 g $(\text{NH}_4)_2\text{HPO}_4$ was added to 50 mL DI water and the pH value of the solution was adjusted to 11 by adding 0.5 mL of 25wt.% ammonia solution. Then the $\text{Ca}(\text{NO}_3)_2$ solution was added dropwise into $(\text{NH}_4)_2\text{HPO}_4$ solution under vigorous stirring in 1 hour. The resultant suspension was stirred (1000 rpm) continuously for further 3 hours in the ice-water bath, and then aged at room temperature for 24 h. The white precipitate was centrifuged and washed repeatedly until neutrality. Finally, the precipitate was freeze-dried and calcined at 500 °C in the air for 4 h to obtain the final HAP support.

2.2 Doping single-atom Pt or Pd on supports and the modification of single-atom with ILs

The Pt/HAP catalysts with 0.2 wt% loadings of Pt were synthesized by a simple impregnation method. In a typical procedure, stoichiometric amounts of PtCODMe_2 (0.2 wt%, compared to HAP support) was added to 5 mL of hexane and sonicated for 3 minutes. Before the addition of HAP to the above Pt precursor solution, HAP was pretreated in the muffle furnace at 100 °C for 1 hour to remove the adsorbed water. The obtained mixture was transferred to the fume hood and stirred at room temperature overnight

to disperse Pt uniformly on HAP and evaporate the excess hexane solvent. Finally, the catalysts were calcined at 100 °C in air for 1 h. To coat ILs on single-atom catalysts, the 0.2Pt/HAP and ILs ([Bmim][Tf₂N], [Bmim][CF₃SO₃], [Bmim][BF₄]) were added to 4 mL methanol, maintaining the molar ratio of Pt to ILs 1:6. The slurry was sonicated for 5 minutes and transferred to fume hood to evaporate the excess methanol with a stirring rate of 500 rpm at room temperature. A similar method was applied to disperse single-atom Pt on CeO₂, TiO₂ and ZrO₂ except that Pt(acac)₂ was used as the precursor and acetone was employed as the solvent. After the evaporation of the solvent, calcination at 200 °C in the air for 1 hour was performed to remove the organic ligand.

Pd single atoms were deposited on HAP by a strong electrostatic adsorption method. Appropriate amount of palladium nitrate was dissolved in 50 mL deionized water, and the pH was adjusted to 10 with 25 vol% ammonia solution. 1 g HAP support was then added to the Pd solution and stirred for 12 h at room temperature. The resulting precipitate was rinsed with deionized water and dried at 80 °C overnight. To modify the prepared Pd/HAP catalyst with [Bmim][BF₄], 0.5 g of Pd/HAP catalysts with 0.02 wt% loading of Pd were dissolved in 4 ml methanol, then 15 mg liquid ionic ([Bmim][BF₄]) was added to the solution followed by sonification for 3 minutes, and the excess methanol was then evaporated with a stirring for about 2 hours at room temperature.

3. Catalyst characterization

High angle annular dark field scanning transmission electron microscopy (HAADF-STEM) images were collected on a FEI Titan 60-300 electron microscope equipped with a spherical aberration corrector. Wide-angle X-ray diffraction pattern (XRD) analysis was performed on a Bruker D8 Advance X-Ray Diffractometer. The measurements were taken at 40 kV applying a potential current of 30 mA and a scan rate of 2°/min from 20 to 80°. *In situ* diffuse reflectance infrared Fourier transform spectroscopy (*in-situ* DRIFTS) study of CO adsorption was carried out on an FTIR spectrometer (Nicolet iS50) equipped with a mercury-cadmium-telluride (MCT) detector that was cooled by liquid nitrogen. Mass flow controllers (Sevenstar, CS200A) were used to control the gas flow rate across the catalyst bed. The DRIFTS were collected in the range of 2300-1800 cm⁻¹ by accumulating 32 scans. Prior to each experiment, 30 mg of the powder samples were loaded into the Harrick high temperature reaction chamber (ZnSe windows) and were purged for 0.5 h with 40 mL/min of pure N₂ at room temperature. The background spectrum that was subtracted automatically from the sample spectrum was recorded in flowing N₂. Then the feed gas containing 5 vol. % CO/Ar was introduced into the chamber with a flow rate of 40 mL/min for 0.5 h. The final CO adsorption spectra were recorded after the purge of 40 mL/min of N₂ for 0.5 h to remove

the gaseous CO. X-ray adsorption spectroscopy (XAS) that include extended X-ray adsorption fine structure (EXAFS) and X-ray fine near-edge structure (XANES) at Pt L₃-edge X-ray were taken at the BL01B1 beamline at SPring-8 (Japan Synchrotron Radiation Research Institute, Hyogo, Japan) in fluorescence mode. Monochromatic X-ray beams were obtained by using a Si (1 1 1) double crystal monochromator which was calibrated at the inflection point of the platinum foil XANES spectrum. Changing glancing angles of collimation and focusing mirrors allowed for the removal of higher harmonics. IFEFFIT and Demeter packages were used as included in Athena and Artemis for the reduction of data. The X-ray edge energy was estimated by using the first maximum of the first derivative of the absorption intensity.

4. Catalytic performance and stability evaluation

The activity of catalysts in hydrogenation of propylene was carried out in a fixed-bed steel tube reactor with length of 200 mm and inner diameter of 8 mm. Mass flow controllers were used to control all gas flows, and the gases (propylene and propane) were analyzed on an Agilent 7890B gas chromatography (GC) equipped with a flame-ionization detector (FID). In each run, 100 mg of catalyst was packed between quartz wool and loaded in the reactor. A feed gas of 30mL/min containing 3 vol.% H₂, 3 vol.% propylene and balance Ar was introduced to the catalyst at room temperature and 1 atmosphere total pressure. Experimental data were collected 30 minutes after the introduction of feed gas to achieve steady-state conditions. Only data reflecting steady-state catalytic reactivity were recorded, and the turnover frequency (TOF) was calculated as moles of propylene consumed per mole of exposed Pt per hour by assuming all Pt atoms of catalysts were accessible to H₂ and propylene molecules. The stability of catalysts in propylene hydrogenation was studied at 90 °C using the same setup. Before the kinetic study, external mass transfer limitations were evaluated by varying the flow rate between 20-40 mL/min at constant weight hourly space velocity (WHSV) under room temperature. The reaction orders with respect to H₂ together with propylene, and activation energy in hydrogenation reaction were measured under the experimental conditions that external mass transfer limitations did not exist. To measure the reaction order in propylene, partial pressure of H₂ was maintained at 0.02 bar and that of propylene was varied from 0.02 to 0.06 bar. For the reaction order in H₂, partial pressure of propylene was kept at 0.02 bar and that of H₂ was changed from 0.005 to 0.03 bar. The activation energy of the catalyst was performed by varying the reaction temperature from 2-25 °C with the same conditions as the catalytic performance test.

The semihydrogenation of acetylene in excess ethylene was conducted in a continuous flow fix-bed reactor. Prior to test, the as-prepared catalysts were in situ reduced in 10 vol% H₂/He with a flow rate of

30 mL min⁻¹ at 100 °C for 0.5h, and then cooled to room temperature. The gas mixture with 2 vol% C₂H₂, 20 vol% H₂, 40 vol% C₂H₄ and He balance was introduced into the reactor with a total flow rate of 30 mL min⁻¹, resulting in a gas hourly space velocity (GHSV) of 2.25 × 10⁸ mL g_{Pd}⁻¹ h⁻¹. The inlet and outlet gas composition were analyzed by GC (A91) with a flame ionization detector (FID) and a Porapak-N column with He as the carrier gas. C₂H₄ and C₂H₆ were the only C2 products detected by GC. Negligible oligomers were formed during the hydrogenation process. Acetylene conversion and selectivity to ethylene were calculated as follows:

$$\text{Conversion} = \frac{\text{C}_2\text{H}_2(\text{feed})-\text{C}_2\text{H}_2}{\text{C}_2\text{H}_2(\text{feed})} \times 100\%$$

$$\text{Selectivity} = \left(1 - \frac{\text{C}_2\text{H}_6-\text{C}_2\text{H}_6(\text{feed})}{\text{C}_2\text{H}_2(\text{feed})-\text{C}_2\text{H}_2} \right) \times 100\%$$

5. Computational details

The calculations were performed by using density functional theory (DFT) with the functional of Perdew, Burke and Ernzerh (PBE)^[1] as implemented in the SIESTA.^[2] The 3d⁷4s¹, 3d³4s¹, 3s²3p⁴, 2s²2p⁴, 2s²2p³, 2s²2p² and 1s¹ of Pt, Ca, P, O, N, C and H atoms are treated for valence electrons, respectively and the remaining core electrons are represented by the Troullier-Martins norm-conserving pseudopotentials.^[3] The calculated lattice parameters of bulk HAP are a = b = 9.42 Å, c = 6.98 Å, which is consistent with the experimental value a = b = 9.41 Å, c = 6.88 Å.^[4] The HAP(001) surface with 3x3x2 element of unit cell is chosen as the computational model. Periodic boundary conditions are used for all systems. All calculations are spin polarized. The energy cutoff of 200 Ry is chosen to guarantee convergence of the total energies and forces. All the calculations were performed at Γ point of the Brillouin zone. The bottom layer is fixed during all the calculations and the other atoms were relaxed. The transition state (TS) is obtained by optimizing the approximate TS which located by double-sphere algorithm^[5] implemented in GRRM17.^[6] All the geometries are visualized by VESTA.^[7]

6. Supporting Experimental Results

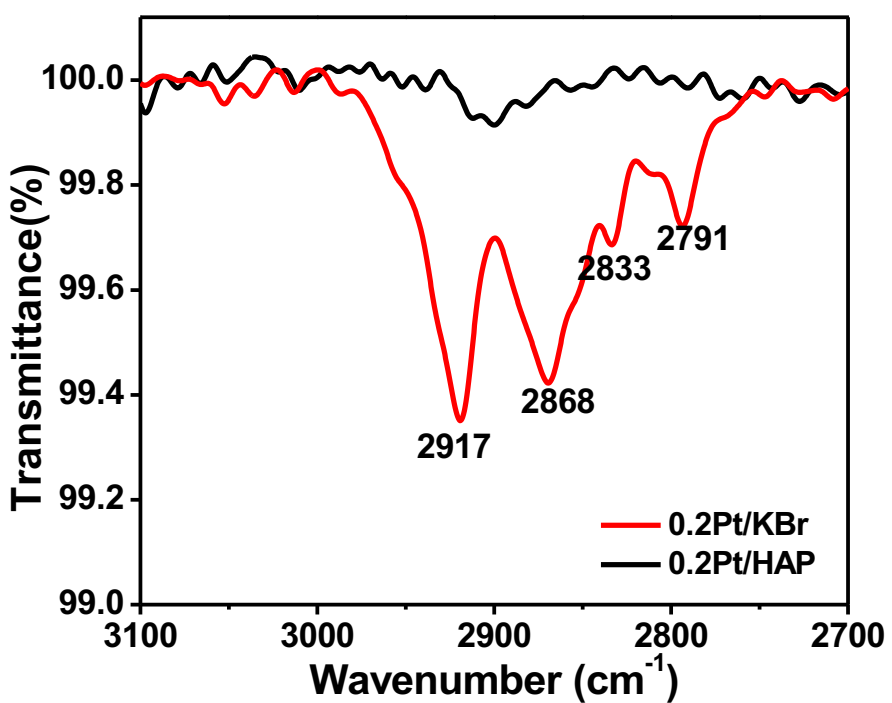


Figure S1. ATR spectra of 0.2Pt₁/HAP that was calcined at 100 °C for 1h in air, and Pt precursor PtCODMe₂ that was diluted with KBr. The Pt percentage for both samples was 0.2 wt.%.

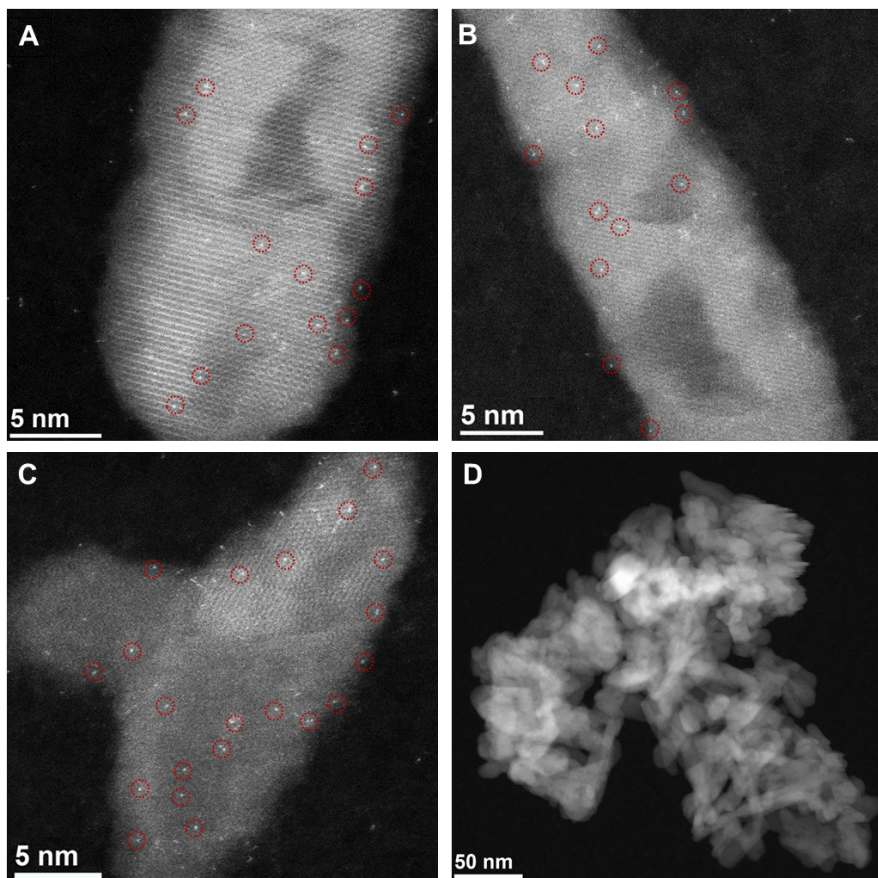


Figure S2. (A-C) HAADF-STEM images and (D) low-magnification HAADF-STEM images of 0.2Pt₁/HAP. To guide the eye, some of the single Pt atoms were circled in red.

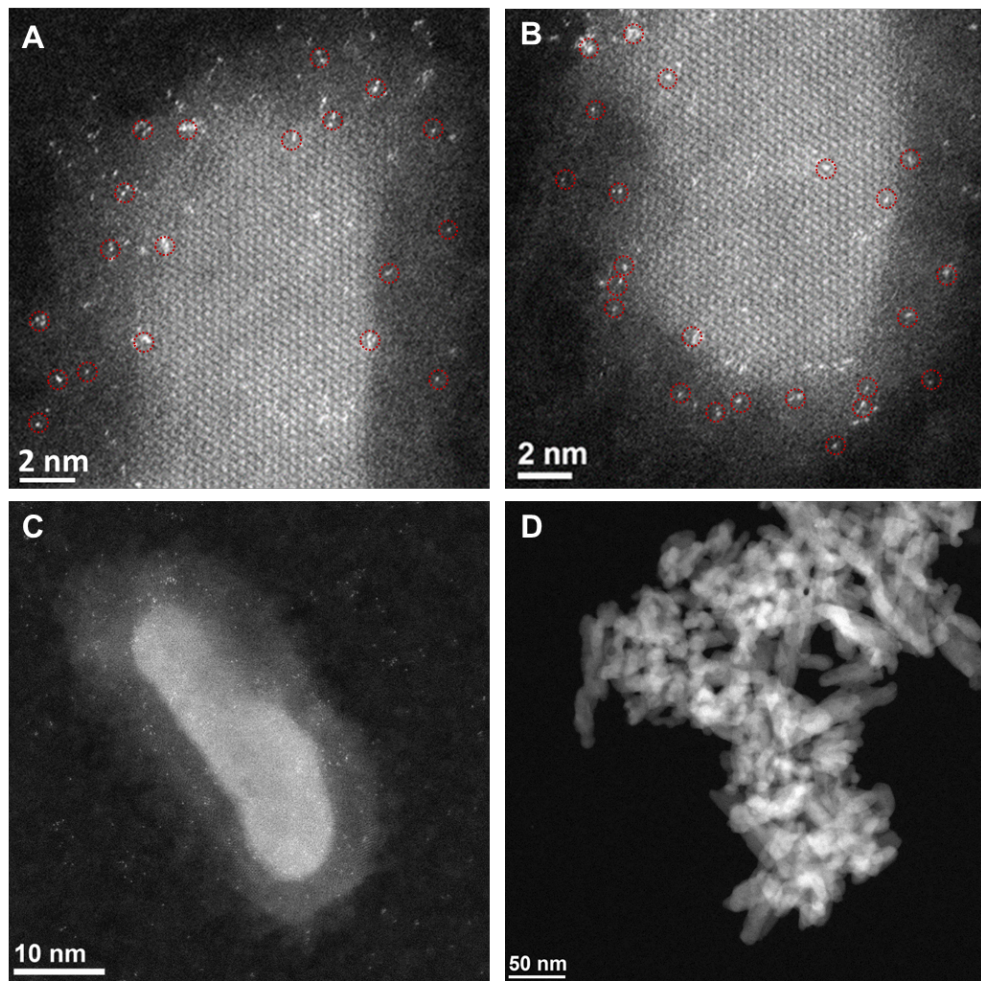


Figure S3. (A-B) HAADF-STEM images and (C-D) low-magnification HAADF-STEM images of BmimTf₂N-0.2Pt₁/HAP.

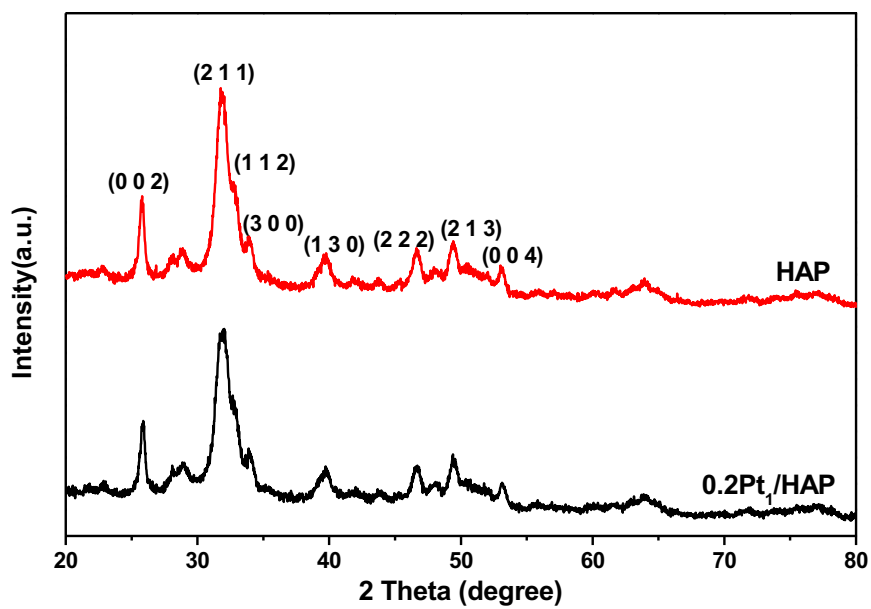


Figure S4. XRD patterns of single-atom 0.2Pt₁/HAP and HAP support.

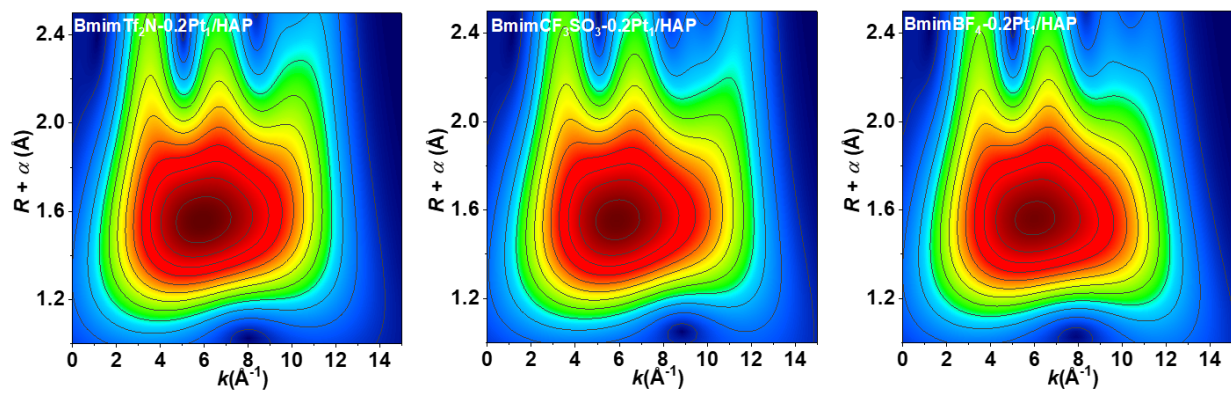


Figure S5. Wavelet transform of the k^3 -weighted EXAFS for ILs-0.2Pt₁/HAP samples.

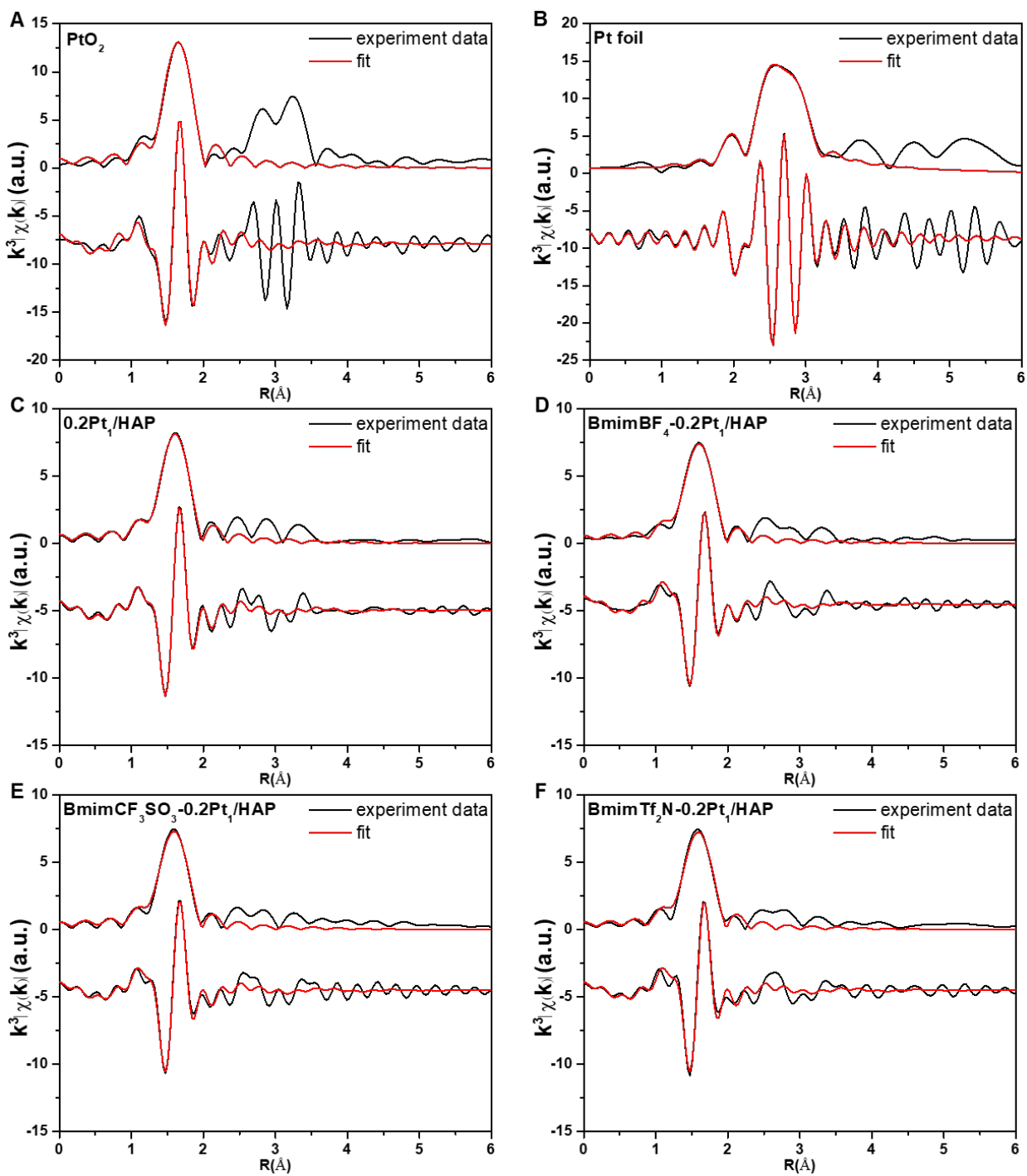


Figure S6. Pt L₃-edge EXAFS spectra and fitting of (A) PtO₂, (B) Pt foil, (C) 0.2Pt₁/HAP, (D) BmimBF₄-0.2Pt₁/HAP, (E) BmimCF₃SO₃-0.2Pt₁/HAP and (F) BmimTf₂N-0.2Pt₁/HAP.

Table S1. EXAFS parameters of 0.2Pt_I/HAP and ILs-0.2Pt_I/HAP.

Samples	Shell	C.N.	R(Å)	$\Delta\sigma^2 \times 10^3(\text{\AA}^2)$	$\Delta E_0(\text{eV})$	r-Factor(%)
Pt foil	Pt-Pt	12(fixed)	2.767±0.002	4.53±0.23	8.47±0.49	0.07
PtO ₂	Pt-O	6(fixed)	2.02±0.007	2.22±0.97	15.00±1.56	0.56
0.2Pt _I /HAP	Pt-O	3.9±0.2	1.998±0.004	3.02±0.46	10.08±0.78	0.12
BmimBF ₄ -0.2Pt _I /HAP	Pt-O	4.2±0.5	2.001±0.009	4.18±1.1	9.12±1.75	0.61
BmimTf ₂ N-0.2Pt _I /HAP	Pt-O	4.0±0.9	1.993±0.015	3.91±1.85	7.87±3.12	1.82
BmimCF ₃ SO ₃ -0.2Pt _I /HAP	Pt-O	4.0±0.6	1.994±0.009	4.02±1.15	8.24±1.90	0.69

C.N, coordination number; R, bond distance; σ^2 , the Debye–Waller factor; ΔE_0 , inner potential correction to account for the difference in the inner potential between the sample and each FEFF simulated path.

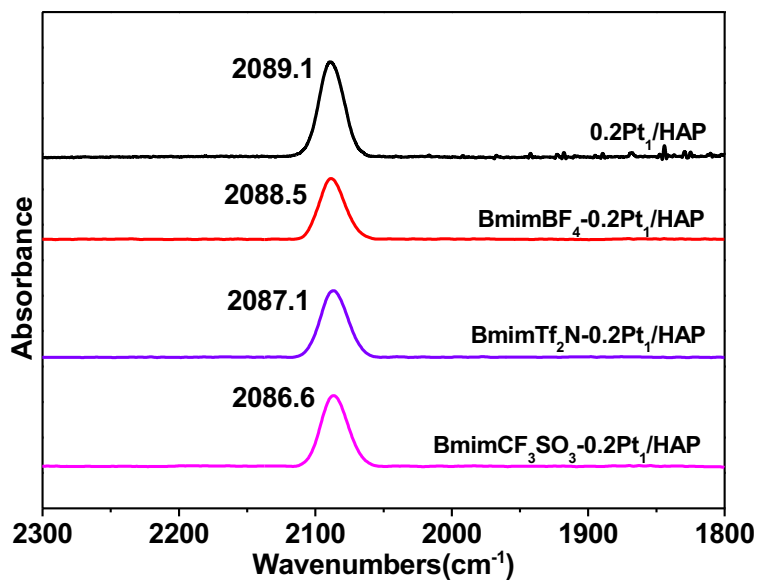


Figure S7. *In situ* FTIR spectra of CO adsorption for 0.2Pt₁/HAP and IL-0.2Pt₁/HAP catalysts.

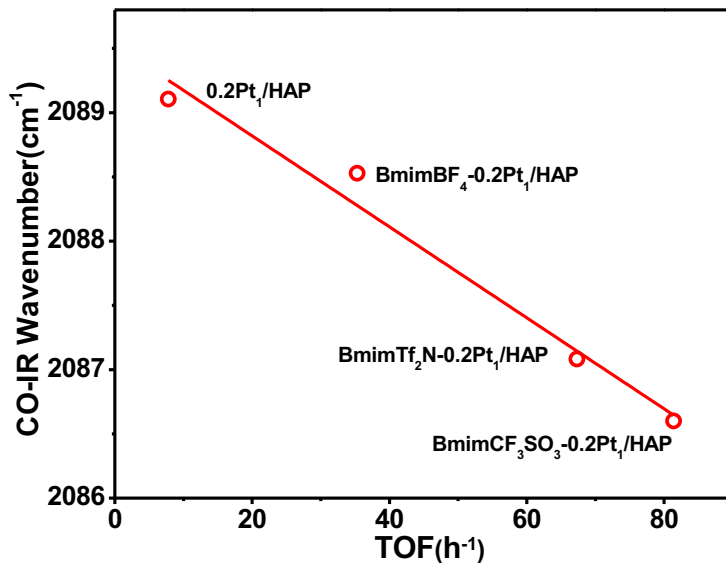


Figure S8. The correlation between TOF during propylene hydrogenation and oxidation state of single-atom Pt.

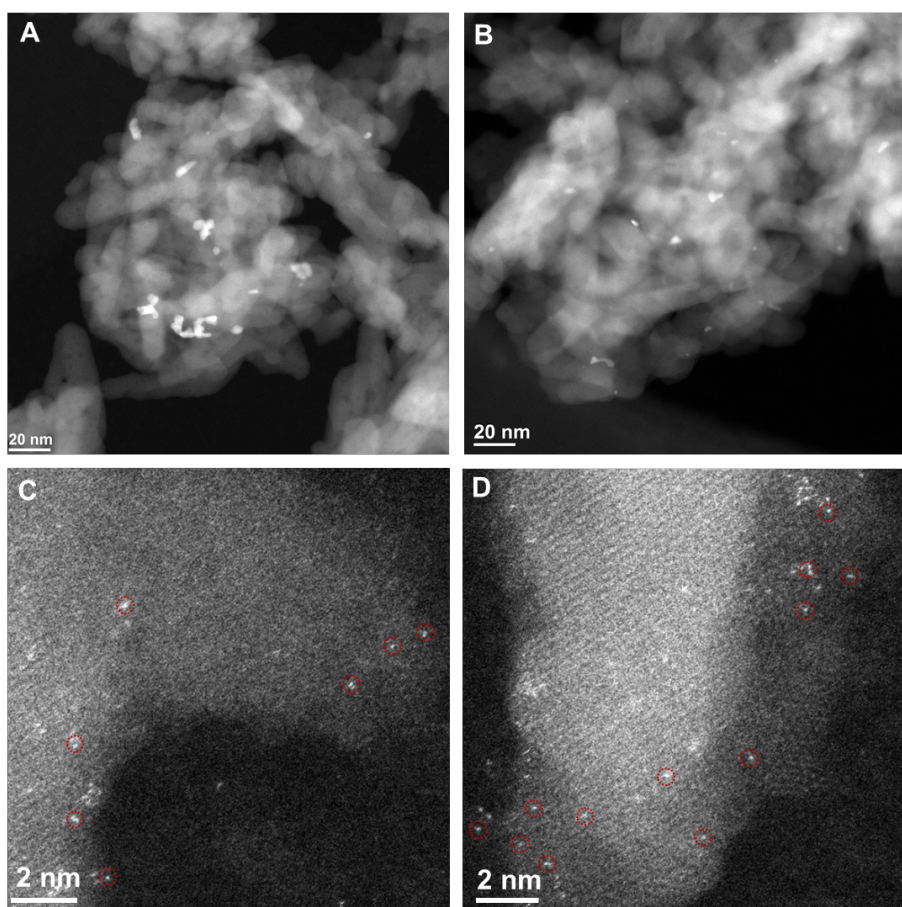


Figure S9. HAADF-STEM images of (A-B) 0.2 Pt₁/HAP and (C-D) BmimTf₂N-0.2Pt₁/HAP after propylene hydrogenation at 90 °C for 1 h.

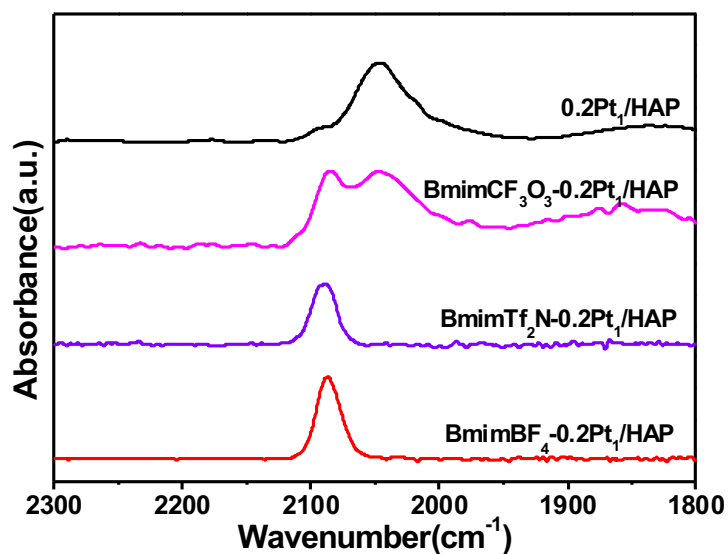


Figure S10. CO adsorption on ILs-0.2Pt₁/HAP catalysts that were reduced in H₂ at 90 °C for 1 hour in 3 vol.% H₂.

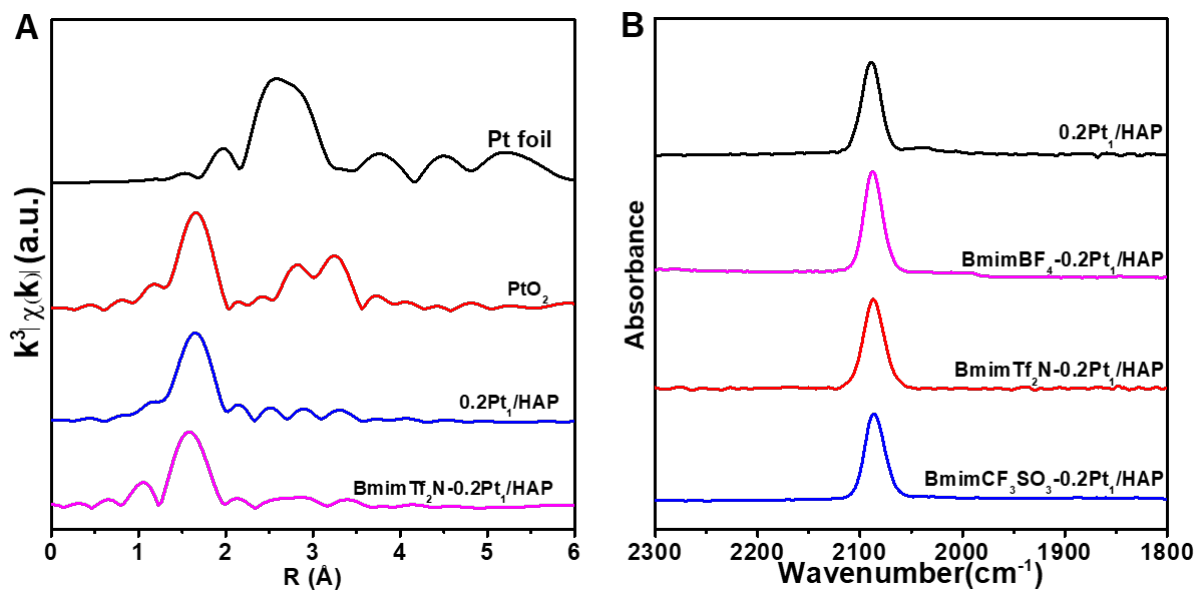


Figure S11. The k^3 -weighted Fourier transform spectra from EXAFS for $0.2\text{Pt}_1/\text{HAP}$ and $\text{BmimTf}_2\text{N}-0.2\text{Pt}_1/\text{HAP}$ after 1 hour of hydrogenation at room temperature (A); In situ FTIR spectra of CO adsorption for $0.2\text{Pt}_1/\text{HAP}$ and ILs- $0.2\text{Pt}_1/\text{HAP}$ after 1 hour of hydrogenation at room temperature with a feed gas of 30 mL/min containing 3 vol.% H_2 , 3 vol.% propylene and balance Ar (B).

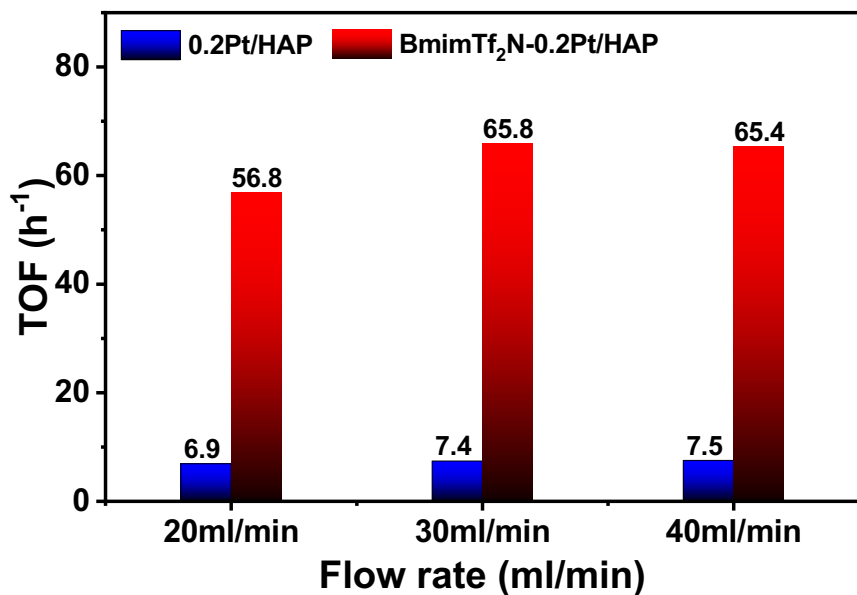


Figure S12. TOF values of propylene over single-atom $0.2\text{Pt}_1/\text{HAP}$ and $\text{BmimTf}_2\text{N}-0.2\text{Pt}_1/\text{HAP}$ at various flow rates with constant space velocity at room temperature.

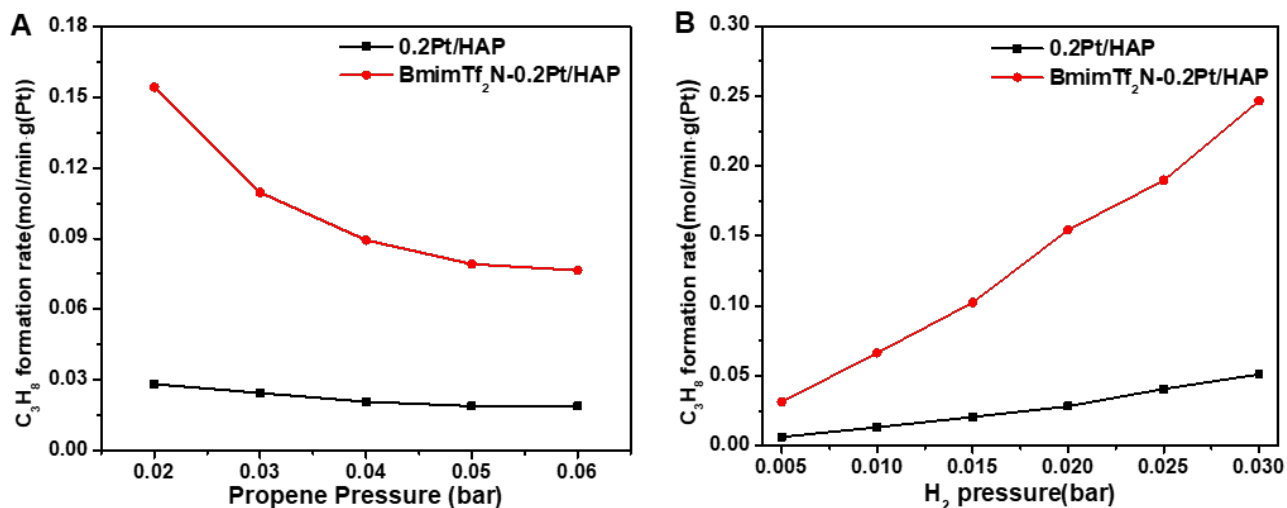


Figure S13. Propylene hydrogenation rates over 0.2Pt₁/HAP and BmimTf₂N-0.2Pt₁/HAP as a function of propylene partial pressure for 0.02 bar of H₂ (A) and a function of H₂ partial pressure for 0.02 bar of propylene (B).

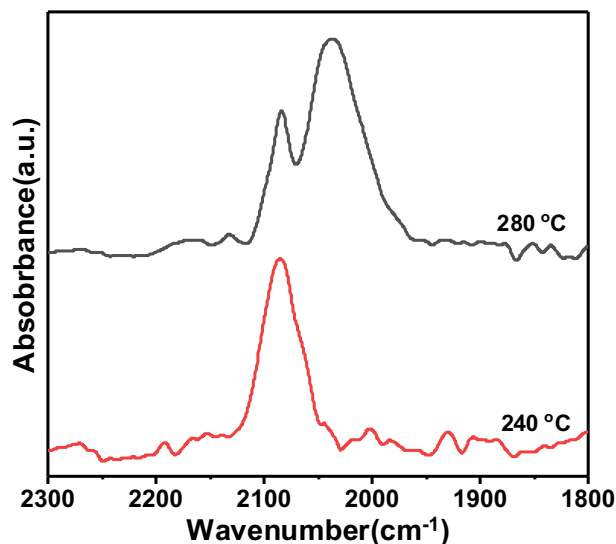


Figure S14. CO adsorption on BmimTf₂N-0.2Pt₁/ZrO₂ catalysts that were reduced in H₂ at 240 and 280 °C, respectively.

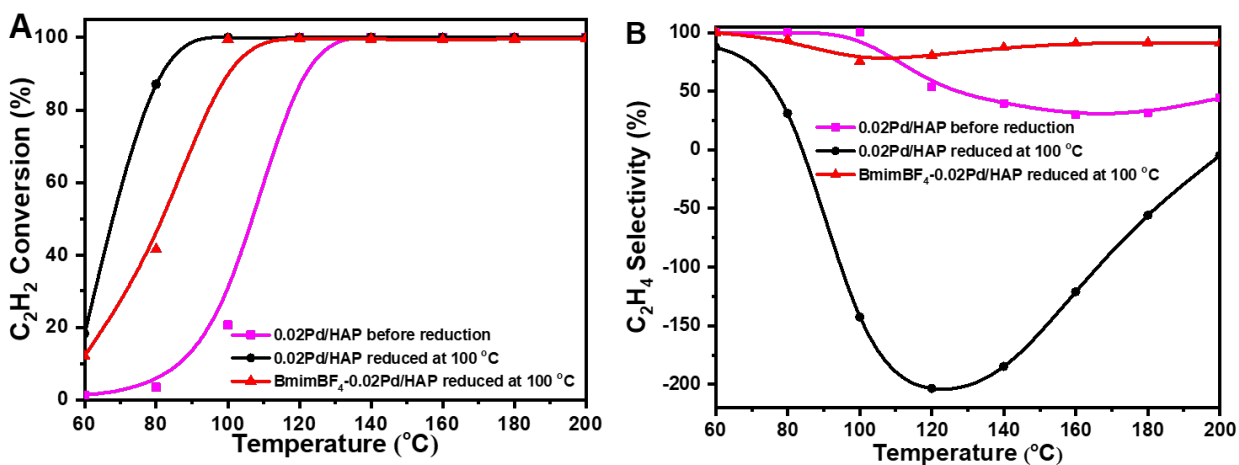


Figure S15. Activity (A) and selectivity (B) during acetylene semi-hydrogenation over 0.02Pd₁/HAP and BmimBF₄-0.02Pd₁/HAP catalysts.

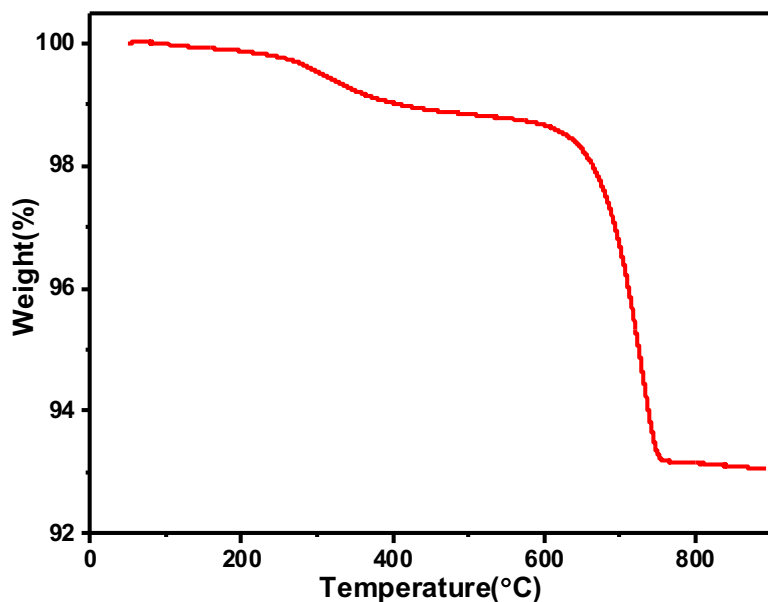


Figure S16. The TG-DTA image of 0.02Pd₁/HAP after acetylene hydrogenation.

References

- [1] J. P. Perdew, K. Burke, and M. Ernzerhof, *Phys. Rev. Lett.* **1996**, *77*, 3865–3868.
- [2] G. Kresse and J. Hafner, *Phys. Rev. B: Condens. Matter Mater. Phys.*, **1993**, *47*, 558–561.
- [3] N. Troullier and J. Martins, *Phys. Rev. B* **1991**, *43*, 1993–2006.
- [4] R.M. Wilson, J.C. Elliott, S.E.P. Dowker *Am. Mineral.* **1999**, *84*, 1406–1414.
- [5] C. Choi, R. Elber, *J. Chem. Phys.* **1991**, *94*, 751–760.
- [6] S. Maeda, Y. Harabuchi, M. Takagi, K. Saita, K. Suzuki, T. Ichino, Y. Sumiya, K. Sugiyama, and Y. Ono, *J. Comput. Chem.*, **2018**, *39*, 233–250.
- [7] K. Momma and F. Izumi: VESTA: a three-dimensional visualization system for electronic and structural analysis, *J. Appl. Crystallogr.*, **2008**, *41*, 653–658.